Iğdır Üniversitesi Fen Bilimleri Enstitüsü Dergisi, 13(3), 1784-1798, 2023
Journal of the Institute of Science and Technology, 13(3), 1784-1798, 2023

ISSN: 2146-0574, eISSN: 2536-4618

Civil Engineering **DOI: 10.21597/jist.1218178**

Research Article

Received: 12.12.2022 **Accepted: 11.05.2023**

To Cite: Aksar, B., Ozdemir, M. A., Tutar, A. I. & Cakir, F. (2023). Structural Analysis of Steel Truss and Masonry Bridge Interaction: A Case of Ali Fuat Pasha Bridge in Sakarya, Türkiye. *Journal of the Institute of Science and Technology*, 13(1), 1784-1798.

Structural Analysis of Steel Truss and Masonry Bridge Interaction: A Case of Ali Fuat Pasha Bridge in Sakarya, Türkiye

Bora AKSAR[1], Muhammed Alperen OZDEMIR[2], Ali Ikbal TUTAR[3], Ferit CAKIR[3*]

Highlights:

- To analyse steel truss and masonry bridge interaction
- To investigate structural performance of Ali Fuat Pasha Bridge
- To examine the combined behavior of steel and masonry materials

Keywords:

- Ali Fuat Pasha bridge
- Masonry bridges
- Steel truss
- Compatibility
- Finite element analyses

ABSTRACT:

Restoration of historical structures using new materials and techniques is widespread worldwide. In these applications, relatively new materials such as steel, concrete, reinforced concrete (RC), or composite are generally preferred. However, it is often ignored whether old materials and new materials work in compatibility. In this respect, Ali Fuat Pasha Bridge (or Bayezid II Bridge), which was built by Bayezid II in 1495 over the Sakarya River in Geyve-Sakarya, was examined. The bridge is 196.50 meters long and consists of 15 arches with different spans and three arches of the bridge were destroyed as a result of the earthquake. Then, the bridge has been restored by constructing a steel truss system in place of the destroyed arches. Within the scope of this study, the structural performance of the bridge, which is currently serving vehicle and pedestrian traffic, is examined by using finite element analyses (FEAs). Moreover, this research examines the combined behavior of steel and masonry materials and investigates the structural behavior of steel truss and masonry bridge interaction. According to the results of the analyses, there are significant behavioral differences between the masonry structure and the steel structure. The main cause for this disparity is thought to be the varying levels of stiffness and ductility in steel and masonry sections.

[1]Bora AKSAR (**Orcid ID:** 0000-0002-9972-5516), Işık University, Faculty of Engineering and Natural Sciences, Department of Civil Engineering, İstanbul, Türkiye

[2]Muhammed Alperen OZDEMİR (**Orcid ID:** 0000-0002-3629-4341), Iğdır University, Faculty of Engineering, Department of Civil Engineering, Iğdır, Türkiye

[3]Ali Ikbal TUTAR (**Orcid ID:** 0000-0003-2577-075X), Ferit CAKIR (**Orcid ID:** 0000-0002-9641-2004), Gebze Technical University, Faculty of Engineering, Department of Civil Engineering, Kocaeli, Türkiye

*** Corresponding Author:** Ferit CAKIR, e-mail: cakirf@gtu.edu.tr

INTRODUCTION

Due to difficult terrain and natural features such as rivers, hollows, and holes, ancient people realized that building bridges was an unavoidable option to overcome these difficulties. They used simple structural forms and natural materials to cross simple openings, while long openings required more engineered systems that could handle structural issues such as large deflections, damaging load concentration points, and stability problems. In ancient times, master builders discovered that arches were an effective way of spanning over long openings, and they could be built relatively easily.

Presently, there are thousands of masonry arch bridges all over the world still carrying heavy traffic, and they play a crucial role in many transportation systems around the globe. These bridges come in various sizes, styles, and spans that reflect different historical civilizations, and they constitute an essential part of the world's cultural heritage. It is crucial that they be preserved for the next generation, and the preservation of these structures is receiving much attention in the structural engineering community. In general, and to the most extent, engineers have relied on several traditional retrofitting techniques that could be implemented for historic bridges. However, traditional retrofitting techniques have sometimes been inadequate for improving these structures' seismic behavior and resistance. Therefore, it is crucial to use materials that have been tested and verified in practice by credible scientific studies and the search for many new materials has begun as an alternative to traditional reinforcement materials. When previous studies are examined, it is understood that research on compatible materials is very limited, and intensive studies are still required on this subject (Aiello et al., 2007; Cancelli et al., 2007; Capozucca, 2010; Grande et al., 2011; Borri et al., 2014).

Table 1. Compatibility of the steel and masonry materials

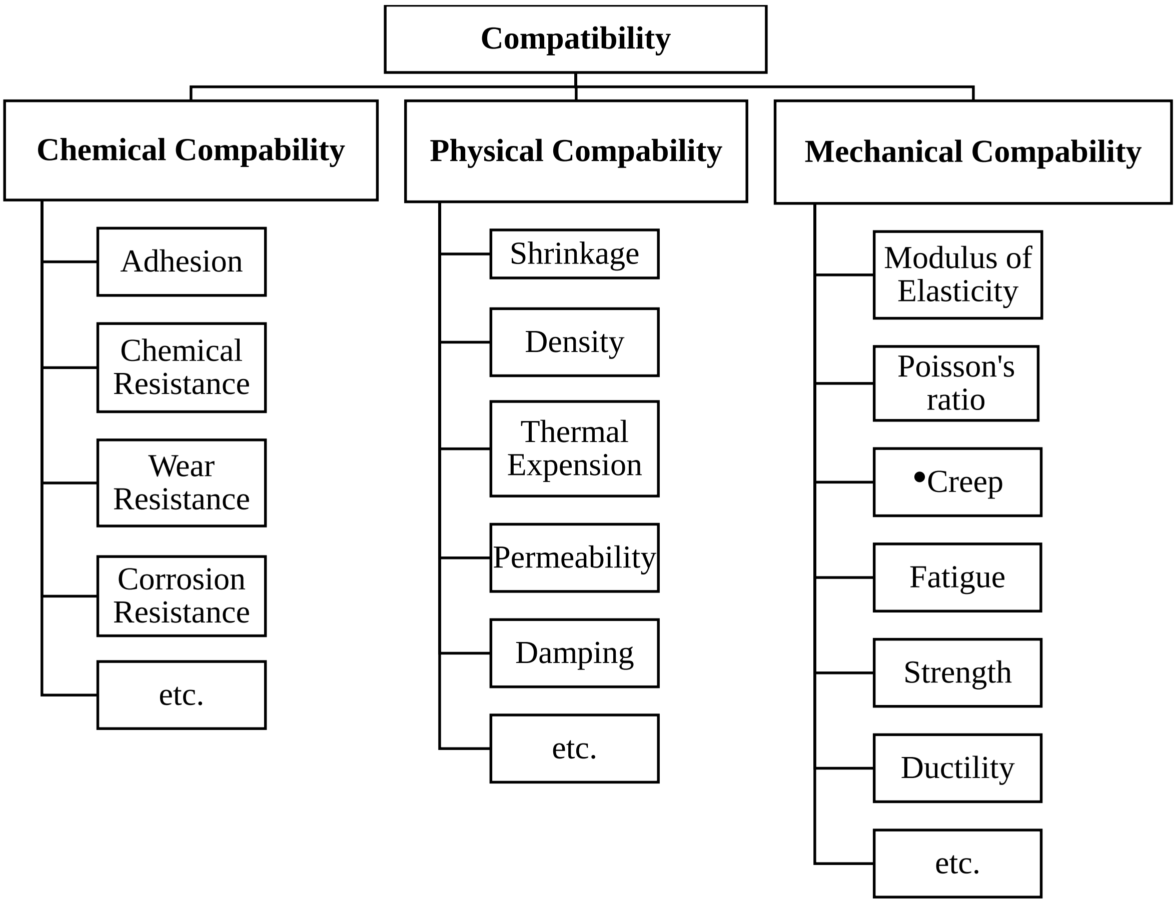

Today, steel materials are typically used for the structural and seismic retrofitting of masonry bridges and many other ancient cultural heritages (Corradi et al., 2018). Steel can be implemented with different construction types and different connection forms in the strengthening and restoration work (Borri et al., 2013; Borri et al., 2014).

Steel and masonry structures are often used together, but it is important to ensure that they are compatible in order to achieve optimal structural performance. Masonry is a brittle material that has limited ductility and low tensile strength, whereas steel is a ductile material with high tensile strength. These differences can lead to compatibility issues between steel and masonry structures. Therefore, engineers must pay close attention to the design and construction process to ensure that the two materials work together seamlessly. Additionally, retrofitting and rehabilitation of masonry structures with steel components require special attention to ensure that the materials are compatible and properly integrated. New research is being conducted to better understand the compatibility between steel and masonry structures, and to develop innovative solutions for retrofitting and rehabilitation that can enhance the performance of these structures while preserving their historical and cultural value.

The structural performance of steel-reinforced masonry structures depends on critical factors such as the strengthening geometry, physical, chemical, and mechanical properties of new and existing materials, compatibility of new and existing materials, and boundary conditions. Compatibility of steel materials with the existing masonry materials is a crucial consideration for the structural performance of the structures. Incompatibility between materials can reduce the durability of either material, making it impossible to use them together. Therefore, structural engineers are increasingly aware of the importance of compatibility between repair systems and existing structures, which can be examined in Table 1.

MATERIALS AND METHODS

Masonry materials, such as stone, have a high modulus of elasticity and are relatively rigid. This rigidity allows them to resist external loads and maintain their shape, but it also means that they are less able to deform or accommodate movement. Steel, on the other hand, is a highly ductile material and can accommodate significant deformations without failing. This ductility allows it to adapt to changes in the environment and work well in combination with other materials. However, when steel is combined with a more rigid material like stone, the steel may undergo large deformations while the masonry remains relatively unchanged. As a result, when a rigid material like stone is combined with a more flexible material like steel, there can be issues with compatibility and deformation. This can result in large stresses in the steel, potentially leading to failure. The interaction between masonry and steel materials also depends on the compatibility of the materials. If the materials are not compatible, such as in the case of dissimilar metals, corrosion can occur, which can weaken the materials over time. Additionally, if the materials have different coefficients of thermal expansion, they may expand or contract at different rates when exposed to temperature changes, which can also lead to stresses and potential failure. the addition of a steel truss system to a stone masonry bridge introduces new challenges due to the differences in behavior between the materials. The rigidity of the masonry and the ductility of the steel can result in compatibility issues, large deformations, and potential failure. It is important to consider these factors when designing and constructing structures that incorporate different materials to ensure their long-term stability and safety. In the study, firstly, information about the general characteristics of steel and masonry materials was given, and then evaluations were made on the Ali Fuat Pasha Bridge.

Structural Steel

In many parts of the world, structural steels of various grades have been produced successfully with the advancement of metallurgical technology over the past few decades. Structural steels are currently manufactured to various specifications to meet various technical requirements and specifications (BS EN 1993-1-1:2005; BS EN 10025-1:2005; ASTM A36/A36M-19; ASTM A572/A572M-21). Structural steel is classified and applied based on its mechanical properties. The chemical composition of steel is an important determinant of mechanical properties, but it is equally important to understand the minimum standards in terms of mechanical strengths and tensile strengths (Table 2 and Table 3). Therefore, it is vitally important for engineers to understand the chemical composition of structural steel, as it will change with specific grades and applications.

Table 2. Chemical compositions of the steel grade tested at 16mm thick (BS EN 10025-2:2019)

Structural Steel Grade	Maximum % carbon (C)	Maximum % manganese (Mn)	Maximum % phosphorus (P)	Maximum % sulfur (S)	Maximum % silicon (Si)
S235	0.22	1.60	0.05	0.05	0.05
S275	0.25	1.60	0.04	0.05	0.05
S355	0.23	1.60	0.05	0.05	0.05

Table 3. Minimum yield strength and tensile strength of the steel grade tested at 16mm thick (BS EN 10025-2:2019)

Structural Steel	Yield Strength (at nominal thickness 16mm) (MPa)	Tensile Strength (at nominal thickness 16mm) (MPa)
S235	235	510
S275	275	530
S355	355	630

Stone

For centuries, stones have been the most important and oldest construction materials for masonry bridges. Therefore, stones are one of the most commonly used materials in traditional masonry bridges. It has been used in regions with local stone availability since the dawn of civilization. Stones that are potentially very solid, durable, and strong have been used to construct masonry bridges. The strength of the stone is also higher than that of other construction materials, but masonry skill and local materials have tended to play a greater role in the construction process. Stone quarrying, selection, weathering, and shaping require skilled and knowledgeable craftsmen because they require a lot of labor. The origin of stones can be classified into genetic systems. There are three major groups according to this system. A list of them is provided in Table 4. Similar masonry structures are made up of the same materials and techniques in the same historic period. Historical masonry structures have been constructed with various stone types by considering their mechanical properties (Table 5 and Table 6). Due to their malleability and softness, sediment stones such as sandstones and limestones have been used in masonry arch bridges for centuries. Even though igneous stones are harder and less malleable than sedimentary stones, they have been used for structures since ancient times. For example, the Romans generally used granite as a masonry building material in the early centuries (Proske & Gelder, 2009).

It is understood that the masonry elements in the Ali Fuat Pasha Bridge were generally built from cretaceous volcanics such as sandstone, siltstone, and limestone. Sandstone is a sedimentary rock that is composed of sand-sized mineral particles, primarily quartz, feldspar, and mica. It is a common building material due to its durability and aesthetic appeal. Sandstone is used in a variety of construction projects, including buildings, bridges, and monuments. Siltstone is a sedimentary rock that is composed of silt-sized mineral particles. It is similar to sandstone but has smaller particles.

Table 4. Classification of stones (Proske & Gelder, 2009)

Major Group	Sub-Group	Examples
	Plutonic	Granite
Igneous	Volcanic	Basanite
	Matrix	Gabbro
	Clastic sediments	Sandstone
Sedimentary	Chemical sediment	Limestone
	Biogenic sediment	Chert
	Residual stones	
Metamorphic		Mica Schist

Table 5. Chemical compositions of the stones (Cressman, 1962; Flower, 1973; Halden & Bowes, 1984; Ghalamghash et al., 2009; Bertetto et al., 2014)

Stones	SiO_2 (%)	Al_2O_3 (%)	K_2O (%)	Na_2O (%)	CaO (%)	FeO (%)
Granite	70-77	11-13	3-5	3-5	1-3	1-3
Basanite	40-45	10-13	1-3	3-5	10-13	8-10
Gabbro	50-55	30-33	0.04-1	3-5	11-14	0.01-1
Sandstone	35-40	10-13	1-3	1-3	5-7	1-4
Limestone	7-11	1-3	0.01-1	0.01-1	45-50	0.01-1
Chert	70-85	10-15	1-3	3-5	0.01-1	3-5
Mica Schist	65-75	10-16	2-5	2-5	1-3	3-6

Table 6. Flexural and compressive strengths of the stones (Schultz, 1995; Zhang et al., 2011; Miskovsky & Seiki, 2011; Kesonen, 2015; Zhu et al., 2020)

Stones	Flexural Strength (MPa)	Compressive Strength (MPa)
Granite	9-15	150-200
Basanite	14-30	250-340
Gabbro	10-24	200-300
Sandstone	3-5	40-50
Limestone	5-25	20-35
Chert	30-45	400-650
Mica Schist	20-30	200-250

Siltstone is often used as a building material because it is relatively durable and easy to work with. Limestone is a sedimentary rock that is composed primarily of calcium carbonate. It is a common building material due to its strength, durability, and natural beauty. Limestone is used in a variety of construction projects, including buildings, bridges, and monuments. It is also used in the production of cement, which is a key component in the construction industry. The steel material, st275, used in the structure is the structural steel material that is frequently used in today's truss systems.

Ali Fuat Pasha Bridge

History of the Structure

Historical Ali Fuat Pasha Bridge, located on the Sakarya River in Ali Fuatpaşa Town, Geyve - Sakarya, was built by Beyazıt-II in 1495 (H.901) according to the historical inscription on the bridge. The bridge and town took their name from Ali Fuat Pasha (Ali Fuat Cebesoy), one of the commanders of the War of Independence. The two arches of the bridge, which were destroyed due to earthquakes, were first rebuilt with a wooden superstructure and in 1949 with a light steel superstructure. Moreover, the bridge was re-restored between 2005-2008 by the General Directorate of Highways in Turkey (Mihladiz & Sancak, 2015).

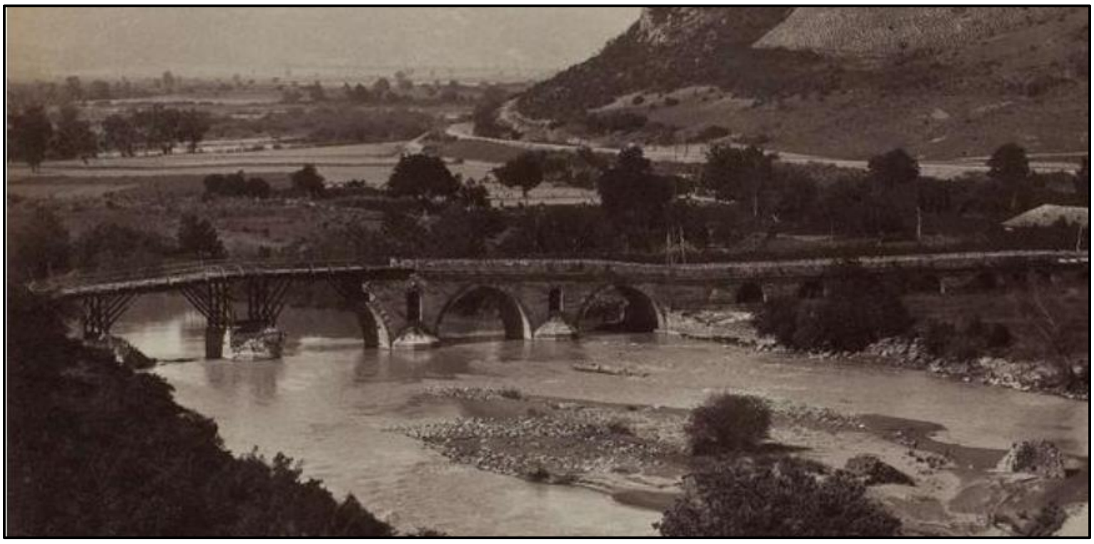

Figure 1. The historical Ali Fuat Pasha bridge in 1888 (Geyveyoresi, 2022)

Geometrical Properties of the Bridge

The bridge, designed by Architect Abdullah, the architect, and engineer of Beyazıt II, is an arched bridge built on fourteen pillars. Four of these piers are located on the Sakarya river, while the others are located on land. This bridge is located on a historical trade road and has a length of 150 meters, a width of 5.60 meters, and a guardrail width of 35 centimeters. In this case, the bridge extends 6.30 meters from the outside to the outside.

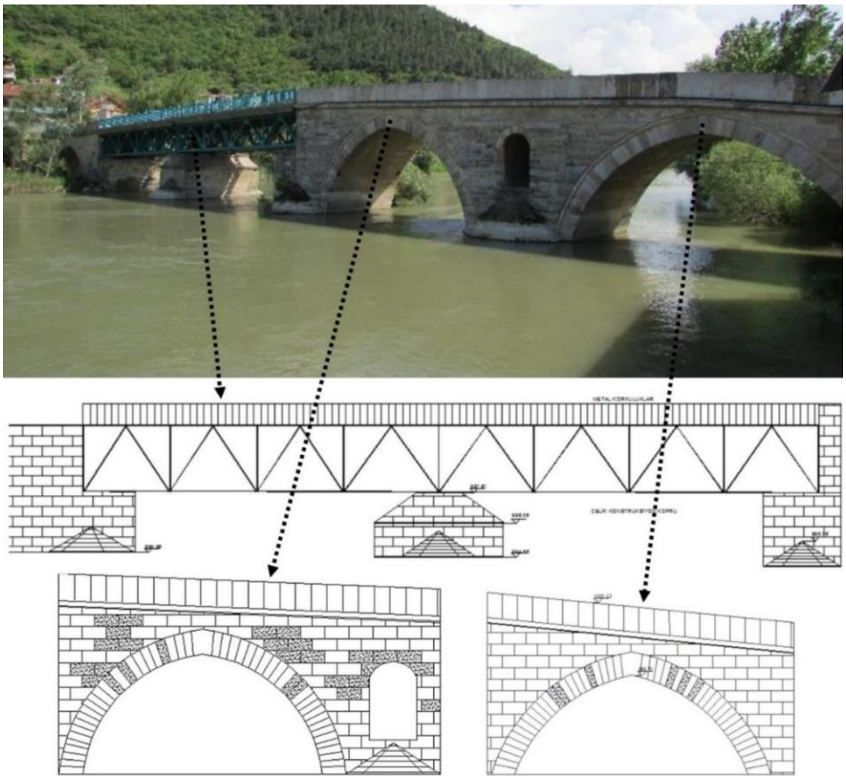

Figure 2. The steel truss and masonry arches of the bridge (Mihladiz & Sancak, 2015)

There are 1.05 meters of guardrails on each side. Two of the fourteen arches of the bridge were later demolished and replaced with steel. There is no masonry part on the steel truss system. In that section, the steel truss section was coated with road section to open the bridge to traffic. The other three-pointed arches are still standing. A total of nine small round arches are located on the land side. In the downstream direction, the floodplains are pentagonal, while in the upstream direction, they are triangular. The number of discharge chambers has been reduced to one today. On the Geyve side of the bridge, the main inscription is located on the back of the mihrab (Geyve, 2022).

Finite Element Analyses (FEAs)

Finite Element Modelling (FEM)

With the development of computer technologies in recent years, it has become common to use a variety of intellectual computer models to solve various problems. A considerable increase has been observed in the number of computer-based studies that use finite-element methods (FEM). This study used a general-purpose finite-element software, ANSYS Workbench (2022), to model masonry arches and steel trusses based on the 3D model. A tetrahedral element shape was preferred in the modeling and solid elements with 20 nodes and 3 degrees of freedom were used. The bridge was modeled with 475718 solid elements and 249090 nodes in the numerical model (Figure 3).

To ensure that the results of an analysis aren't affected by changes in the mesh size, the convergence of the mesh determines how many elements must be included in the model. The system response (stress, deformation) becomes repeatable as the element size decreases. In this study, through mesh convergence analysis, it is demonstrated that an iterative method leads to a correct FEA solution. By varying the number of elements along each edge, the maximum vertical deflection was measured against mesh size versus deflection and solution time. As a result, the mesh size and mesh quality used in the study were determined by this approach.

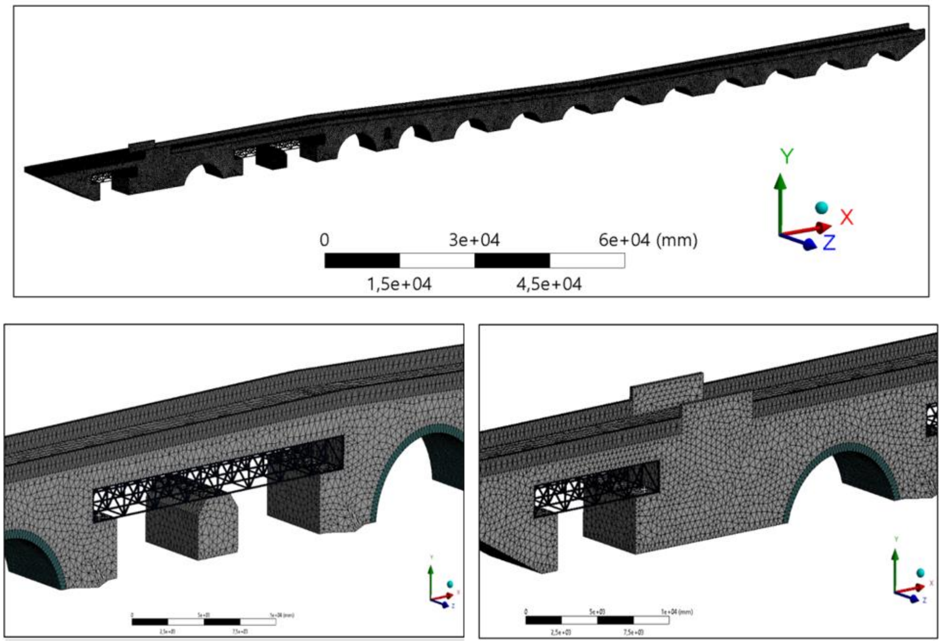

Figure 3. The FEM of the bridge

In this finite element model and analysis, the following variables and assumptions were used:

- To reduce modeling errors, certain architectural features that do not affect structural performance have been ignored to make it easier to see the results of the analysis.

- Material properties were used according to Table 7.
- Foundation nodes were assumed to be fixed.
- A total of 30 modes were considered in the modal analysis.
- The connections between the steel truss system and the masonry structure were considered bonded connections.

Table 7. Mechanical properties of the materials (Cakir and Seker, 2016; Cakir, 2018; Varro et al., 2021)

Structural Components	Density (kg/m3)	Poisson's Ratio	Young Modulus (MPa)
Masonry Spandrel	2200	0.18	20000
Masonry Arch	2300	0.18	27650
Masonry Parapet	1860	0.19	18700
Steel Truss	7850	0.30	200000

Static Analysis

In the first step, the static analysis was performed to obtain the static performance, taking a static load into account for dead loads. For static analyses, vertical displacements and critical stresses were calculated for bridges subjected to static forces. As expected, the maximum displacement occurred on the center of the steel bottom chord (tie beam) and was about 0.68 mm (Figure 4). The analysis resulted in a maximum principal stress of 13.36 MPa (Figure 5). Furthermore, the minimum principal stresses were found to be -44.31 MPa above the bottom of the steel column (king post) (Figure 6). The maximum and minimum principal stresses occurred at the connection section between the steel rods and the transition zone between the masonry walls and the steel truss (Figure 5 and Figure 6).

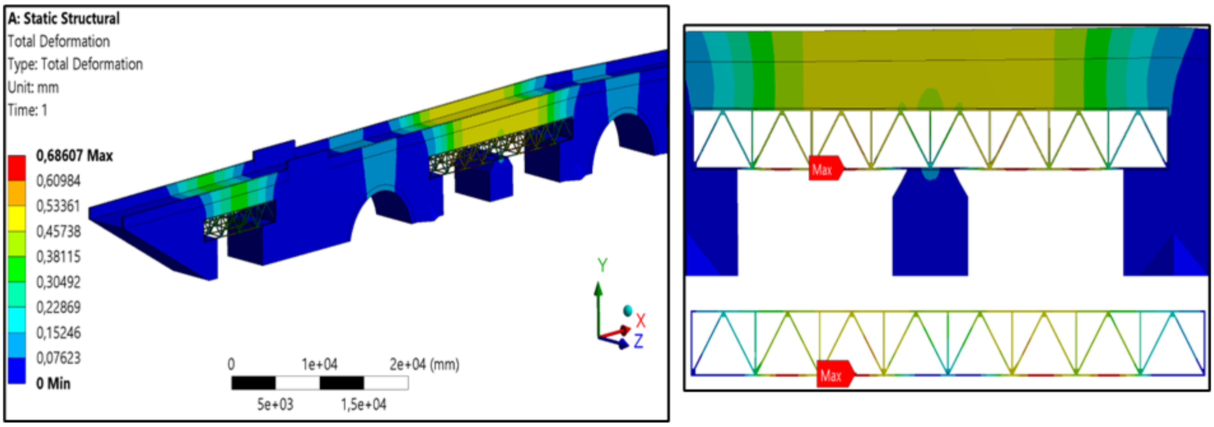

Figure 4. Total deformation obtained from the static analysis (mm)

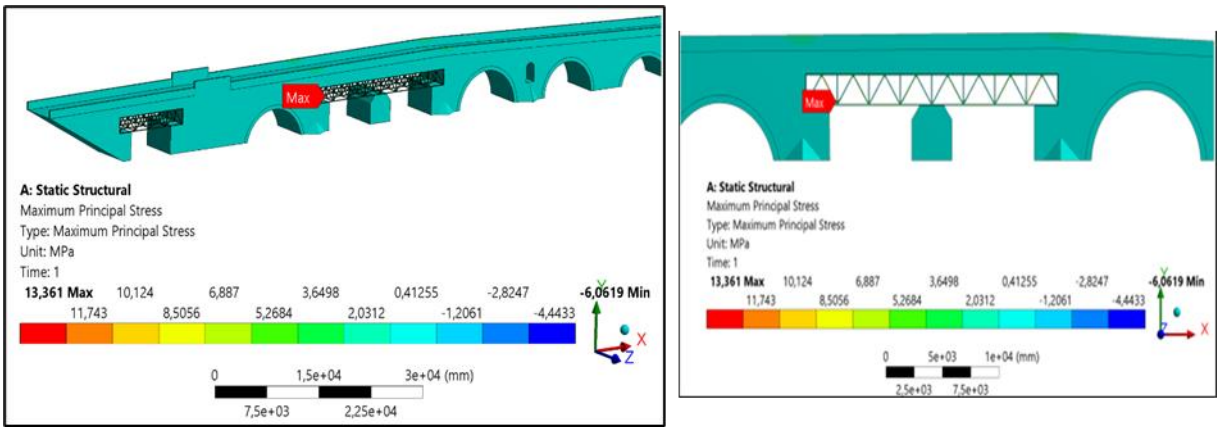

Figure 5. Maximum principal stress obtained from the static analysis (MPa)

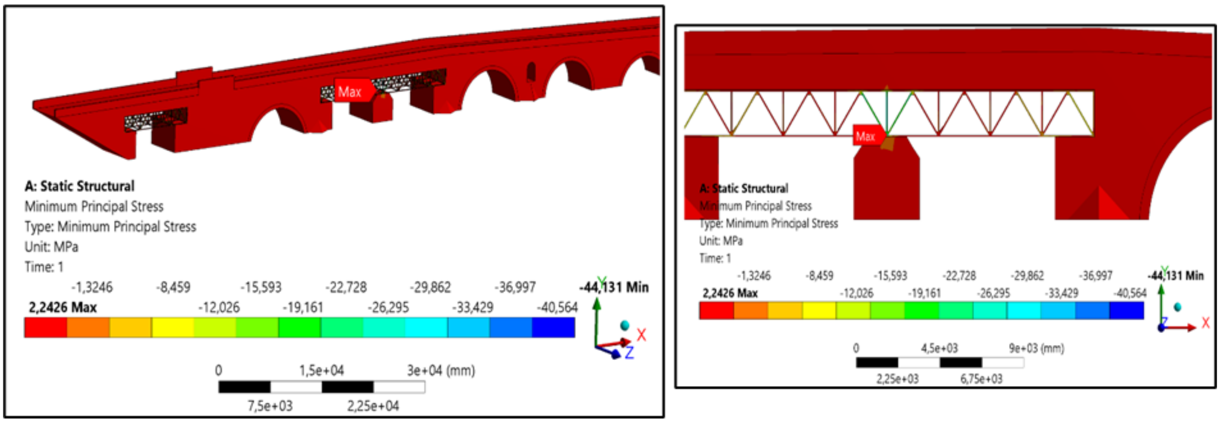

Figure 6. Minimum principal stress obtained from the static analysis (MPa)

Modal Analysis

Table 8. The frequencies and mass participation of the first six modes

	MODE	FREQUENCY	PERIOD	PARTIC.FACTOR	RATIO	EFFECTIVE MASS	CUMULATIVE MASS FRACTION	RATIO EFF. MASS TO TOTAL MASS
X-DIRECTION	1	16.2722	0.61455E-01	-0.25358E-02	0.004876	0.643024E-05	0.235881E-04	5.65E-10
	2	18.0422	0.55426E-01	0.18886E-01	0.036314	0.356681E-03	0.133200E-02	3.13E-08
	3	18.3034	0.54635E-01	-0.34938E-02	0.006718	0.122063E-04	0.137678E-02	1.07E-09
	4	19.0244	0.52564E-01	-0.31208E-02	0.006001	0.973944E-05	0.141251E-02	8.56E-10
	5	23.7903	0.42034E-01	0.52007	1.000000	0.270473	0.993589	2.38E-05
	6	27.3118	0.36614E-01	-0.41804E-01	0.080382	0.174760E-02	1.00000	1.54E-07
Y-DIRECTION	1	16.2722	0.61455E-01	-0.32836E-01	0.001538	0.107823E-02	0.236598E-05	9.48E-08
	2	18.0422	0.55426E-01	-0.49896E-04	0.000002	0.248964E-08	0.236598E-05	2.19E-13
	3	18.3034	0.54635E-01	0.16499E-01	0.000773	0.272228E-03	0.296334E-05	2.39E-08
	4	19.0244	0.52564E-01	-0.11367E-01	0.000532	0.129218E-03	0.324688E-05	1.14E-08
	5	23.7903	0.42034E-01	21.348	1.000000	455.722	0.999998	4.01E-02
	6	27.3118	0.36614E-01	0.28751E-01	0.001347	0.826596E-03	1.00000	7.26E-08
Z-DIRECTION	1	16.2722	0.61455E-01	26.747	1.000000	715.399	0.824275	6.29E-02
	2	18.0422	0.55426E-01	-0.29948	0.011197	0.896891E-01	0.824378	7.88E-06
	3	18.3034	0.54635E-01	-8.8323	0.330216	78.0090	0.914260	6.86E-03
	4	19.0244	0.52564E-01	2.1264	0.079501	4.52165	0.919469	3.97E-04
	5	23.7903	0.42034E-01	0.36901E-01	0.001380	0.136171E-02	0.919471	1.20E-07
	6	27.3118	0.36614E-01	8.3602	0.312565	69.8922	1.00000	6.14E-03

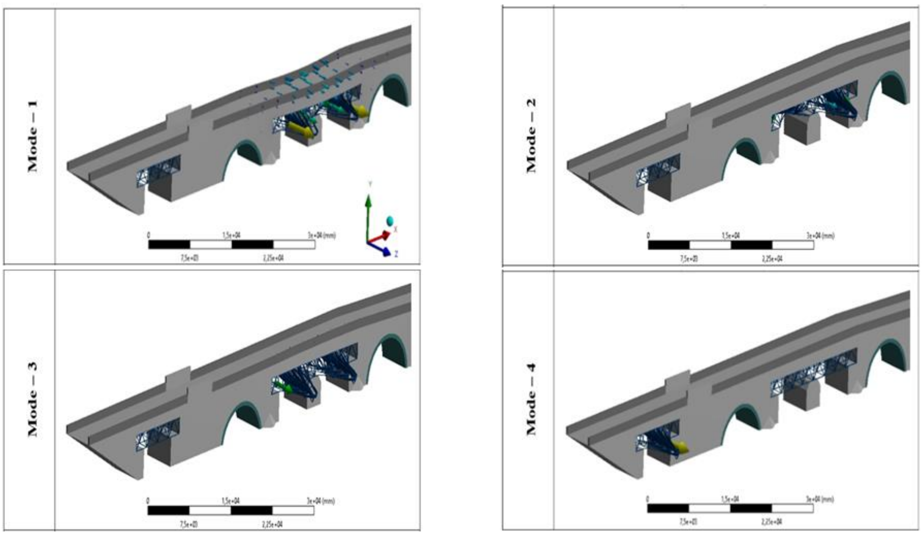

Figure 7. The first four mode shapes of the structure

To determine the free vibration periods, mode shapes, and modal mass participation ratios, modal analysis was performed considering 112 modes, and the first six modes were examined. According to the analysis, the modal mass participation ratios in the structure's X, Y, and Z directions reached 96.91%, 95.06%, and 96.19%, respectively. For the first six modes, the obtained frequencies, periods, and effective mass participation ratios are given in Table 8, and the first four mode shapes are shown in Figure 7. As can be seen from the first six mode shapes, the modal behavior of the steel truss system has a dominant character over the behavior of the bridge.

Response Spectrum Analysis

It is both a challenging and significant problem to assess the seismic performance of a heritage building. Thus, masonry structures located in active seismic zones need to be tested for earthquake performance. According to the Turkish Disaster and Emergency Management Presidency (AFAD), Sakarya is situated in a first-degree (one of the most dangerous) earthquake-prone zones in which the peak ground acceleration (PGA) corresponding to the design earthquake level is expected to exceed 0.4 g. Consequently, earthquakes are one of the major problems for the Ali Fuat Pasha Bridge in Sakarya, Turkey. No experimental work has been done on the ground. However, due to the general geological structure of Sakarya province and the bridge being built on the stream bed, the ZC soil type was accepted as the soil type. The response spectrum was selected based on the ZC soil type using the Turkish Earthquake Hazard Map (AFAD, 2022) (Figure 8) and Ss, S_1, PGA, and PGV are 1.134, 0.325, 0.463 g, and 30.081 cm/s, respectively.

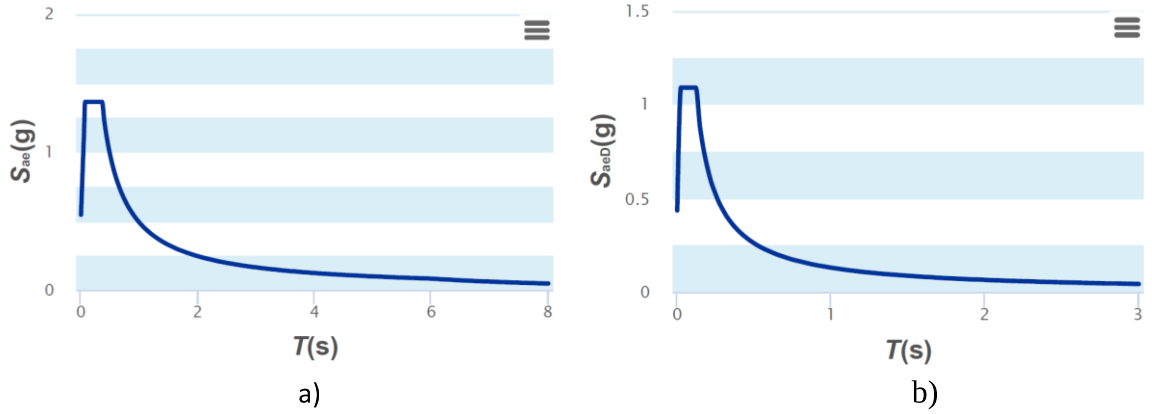

Figure 8. The elastic design spectrums, a) vertical, b) horizontal (AFAD, 2022)

The bridge was evaluated based on simulated ground records for a 475-year return period (DD2: Probability of occurrence in 50 years is 10%). Based on the DD2-seismic hazard level, the performance evaluation was conducted by using the response spectrum analysis. Response spectrum analyses were performed in both horizontal directions; X and Z directions.

Out-of-plane (Z direction) Analysis

First of all, out-of-plane (Z direction) analysis was performed, where the structure showed poor behavior. Figure 9 shows the maximum horizontal displacement based on the response spectrum analysis in the Z direction. As shown in Figure 9, the maximum lateral displacements around the steel truss tie beam were 7.04 mm. As shown in Figure 10, the maximum normal stress around the connection section of the masonry main structure and the steel truss was 53.653 MPa. As a result of the analysis, shear stresses were also examined. The stresses formed by considering different planes in shear stresses were investigated. When the shear stresses occurring in the XY, XZ, and YZ planes are examined, it is seen that the shear stresses occur intensely at the nodal points of the steel truss system and the connection points of the steel truss system with the masonry walls. Considering the maximum stresses obtained, it was determined that the values of 27.509 MPa, 17.09 MPa, and 16.603 MPa were reached in the XY, XZ, and YZ planes, respectively (Figure 11-13).

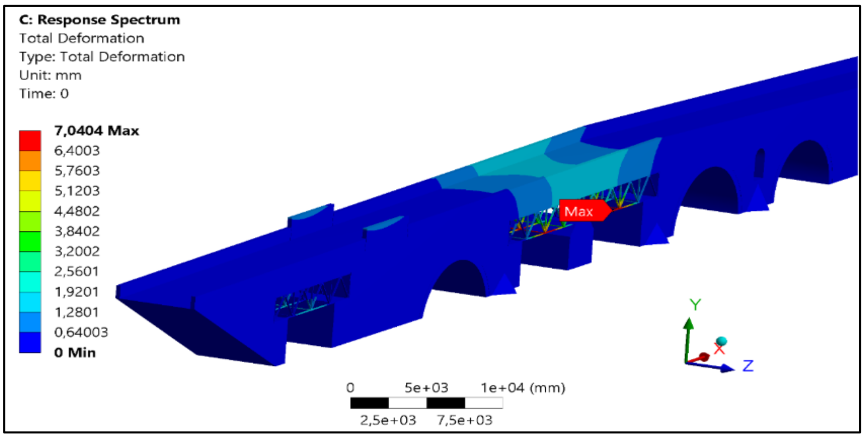

Figure 9. Total deformation obtained from the response spectrum analysis in the Z Direction (mm)

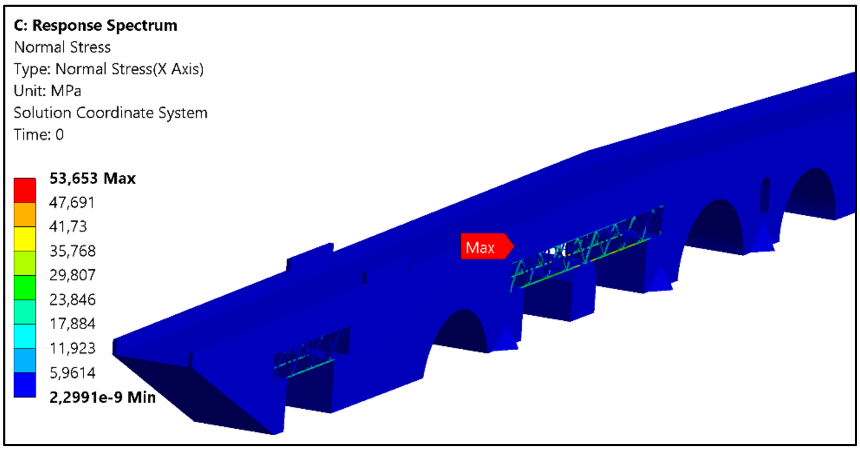

Figure 10. Normal stress obtained from the response spectrum analysis in the Z direction (MPa)

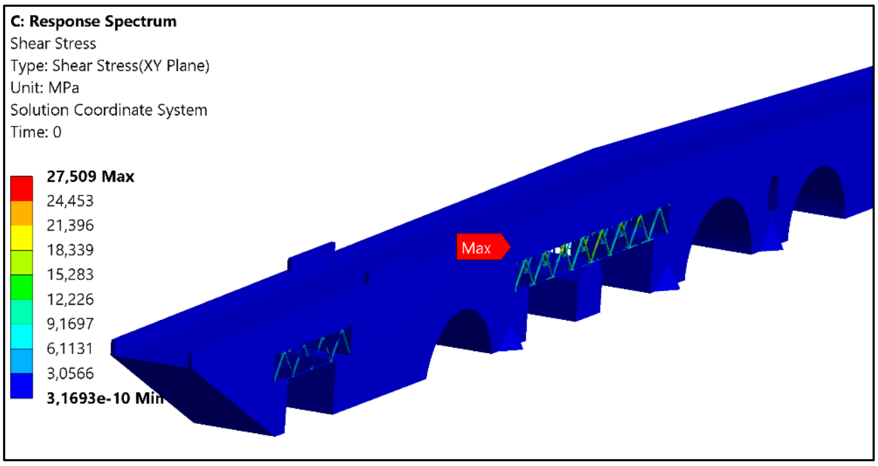

Figure 11. Shear stress (XY Plane) obtained from the response spectrum analysis in the Z direction (MPa)

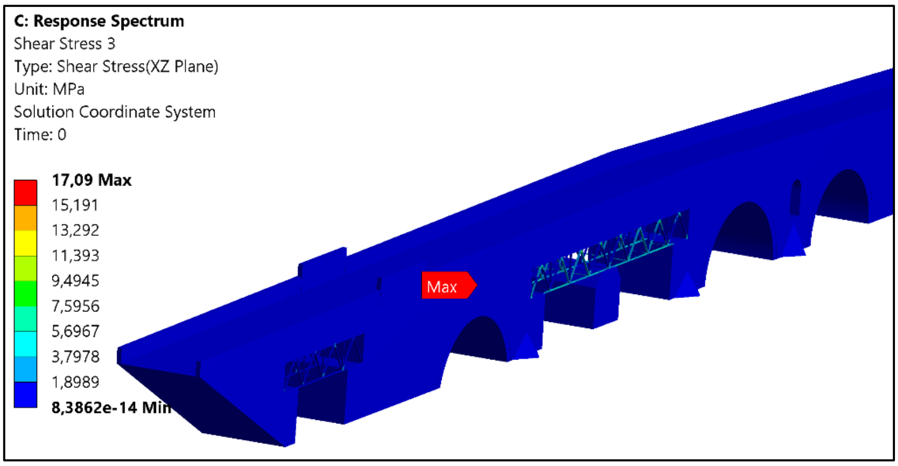

Figure 12. Shear stress (XZ Plane) obtained from the response spectrum analysis in the Z direction (MPa)

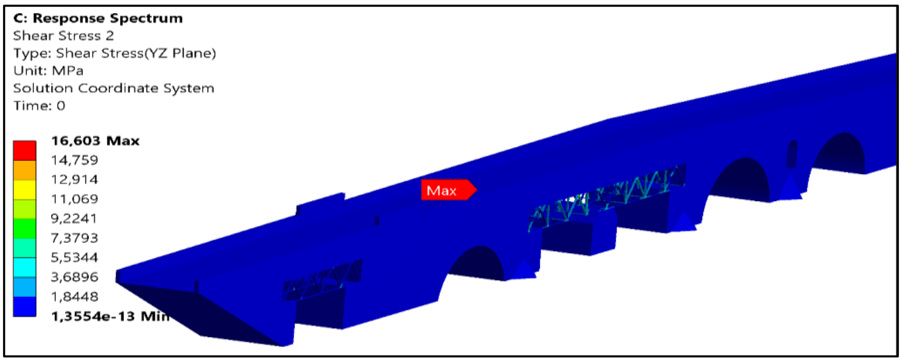

Figure 13. Shear stress (YZ Plane) obtained from the response spectrum analysis in the Z direction (MPa)

In-plane (X direction) Analysis

In the second part, in-plane (X direction) analyzes were performed. Based on the response spectrum analysis in the X direction. The steel truss tie beam experienced maximum lateral displacements of 3.0227 mm, as indicated in Figure 14. Moreover, Figure 15 demonstrates that the maximum normal stress was 52.938 MPa around the connection section of the masonry main structure and the steel truss. In addition to normal stresses, shear stresses were also examined by considering different planes. It was observed that shear stresses occurred predominantly at the nodal points of the steel truss system and the connection points of the steel truss system with the masonry walls in the XY, XZ, and YZ planes. Figures 16 to 18 show that the maximum stresses reached were 43.787 MPa, 51.635 MPa, and 50.797 MPa, respectively.

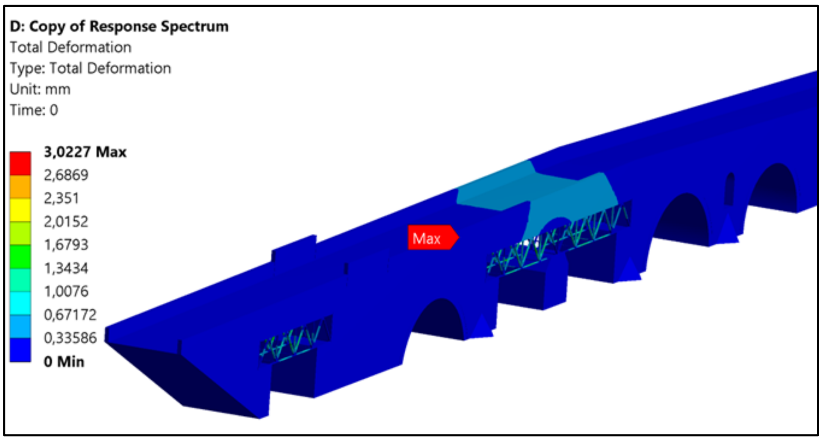

Figure 14. Total deformation obtained from the response spectrum analysis in the X Direction (mm)

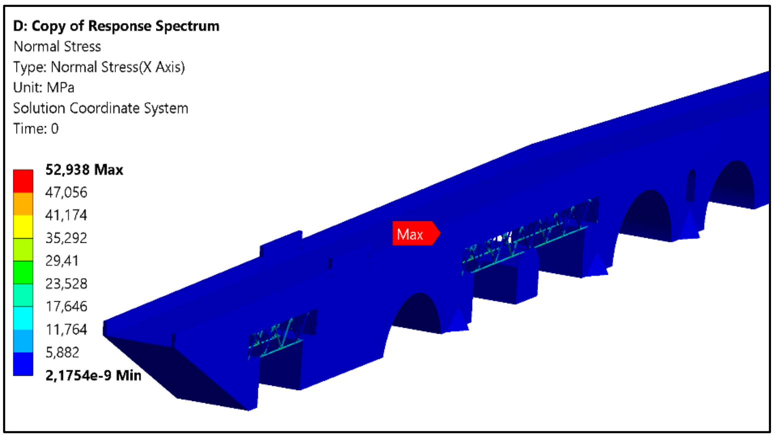

Figure 15. Normal stress obtained from the response spectrum analysis in the X direction (MPa)

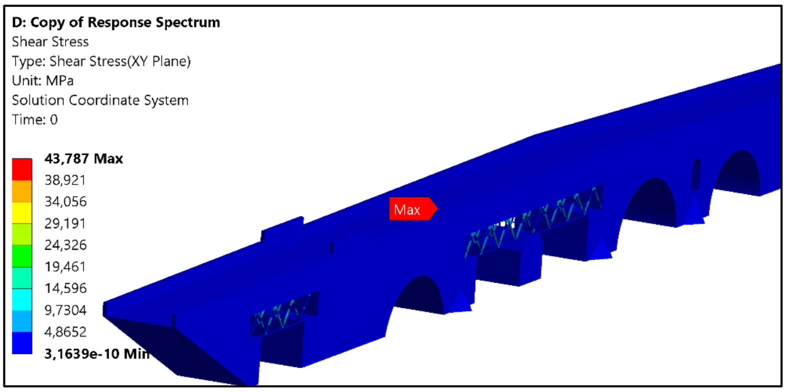

Figure 16. Shear stress (XY Plane) obtained from the response spectrum analysis in the X direction (MPa)

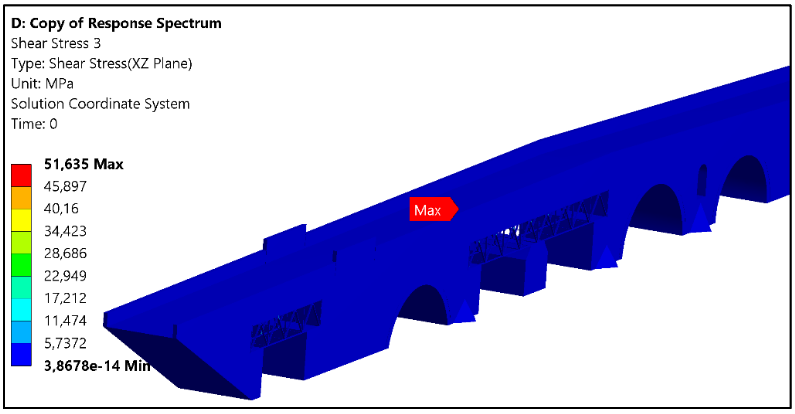

Figure 17. Shear stress (XZ Plane) obtained from the response spectrum analysis in the X direction (MPa)

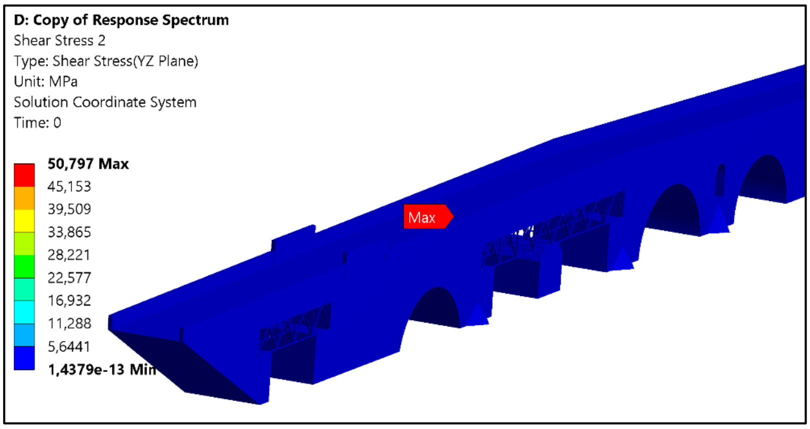

Figure 18. Shear stress (YZ Plane) obtained from the response spectrum analysis in the X direction (MPa)

CONCLUSION

Ancient people were forced to build bridges to overcome difficult terrain and earth features, such as rivers, hollows, and holes. Natural materials and simple structural forms were used for crossing simple openings. Large openings, however, require more engineered systems that can handle structural issues such as large deflections, damaging load concentration points, and stability concerns. Arches were discovered to be an effective way of spanning over long-span openings during ancient times, and they were relatively easy to construct. Nowadays, thousands of these masonry arch bridges are still carrying heavy traffic around the world, and they play a crucial role in many transportation systems.

Several critical factors affect the structural performance of steel-reinforced masonry structures, including (1) strengthening geometry, (2) physical, chemical, and mechanical properties of new and existing materials, (3) compatibility between new and existing materials, and (4) boundary conditions. In these factors, the compatibility of steel materials with existing masonry materials plays a crucial role in determining structural performance. As a result of the evaluation of the analyzes made, it is seen that there is a serious behavioral difference between masonry structures and steel structures. Here, the most important difference is thought to be the difference in stiffness and ductility in steel and masonry elements. For this reason, it is suggested that these differences should be considered in the reinforcement or additional section designs to be made with steel materials on masonry structures.

Conflict of Interest

The article authors declare that there is no conflict of interest between them.

Author's Contributions

The authors declare that they have contributed equally to the article.

REFERENCES

AFAD, (2022). Republic of Turkey Prime Ministry, Disaster and Emergency Management Presidency, Earthquake Department, https://tdth.afad.gov.tr/TDTH/main.xhtml

Aiello, M. A., Micelli, F., Valente, L. (2007). Structural upgrading of masonry columns by using composite reinforcements. *Journal of Composites for Construction*, 11:650–658. doi: 10.1061/(asce)1090-0268(2007)11:6(650)

ANSYS Workbench, 2022. Finite Element Software, US.

ASTM A36/A36M-19. Standard Specification for Carbon Structural Steel. 100 Barr Harbor Drive, PO Box C700, West Conshohocken, PA: ASTM International.

ASTM A572/A572M-21. Standard Specification for High-Strength Low-Alloy Columbium-Vanadium Structural Steel. 100 Barr Harbor Drive, PO Box C700, West Conshohocken, PA: ASTM International.

Bertetto A. M., Grosso, B., Ricciu, R., Rizzu, D. (2014). Anisotropic and impulsive neutron emissions from brittle rocks under mechanical load. *Meccanica*, 50:1177–1188. doi: 10.1007/s11012-014-9987-9

Borri, A., Castori, G., Corradi, M. (2013). Masonry confinement using steel cords. *Journal of Materials in Civil Engineering*, 25:1910–1919. doi: 10.1061/(asce)mt.1943-5533.0000753

Borri, A., Castori, G., Corradi, M. (2014). Strengthening of fair face masonry columns with steel hooping. *Materials and Structures*, 47:2117–2130. doi: 10.1617/s11527-014-0376-6

BS EN 10025-1:2005. Hot rolled products of structural steels: Part 1: General technical delivery conditions. London: British Standards Institution.

BS EN 10025-2:2019 Hot rolled products of structural steels Technical delivery conditions for non-alloy structural steels. London: British Standards Institution.

BS EN 1993-1-1:2005. Eurocode 3, Design of Steel Structures: Part 1-1: General rules and rules for buildings. London: British Standards Institution.

Cakir, F. (2018). Structural Performance Assestment of Historical Dilovasi Sultan Suleyman (Diliskelesi) Bridge in Turkey, *International Journal Of Electronics, Mechanical And Mechatronics Engineering*, Vol.8 Num.3 - 2018 (1579-1588)

Cakir, F., Şeker, B.S. (2015). Structural performance of renovated masonry low bridge in Amasya, Turkey, *Earthquakes and Structures*, Vol. 8, No. 6 (2015) 1387-1406 doi: 10.12989/eas.2015.8.6.1387

Cancelli, A. N., Aiello, M. A. and Casadei, P. (2007). Experimental investigation on bond properties of SRP/SRG-Masonry systems. T.C. Triantafillou, ed., Proc., Fiber-Reinforced Polymer Reinforcement for Concrete Structures (FRPRCS-8), Patras, Greece

Capozucca, R. (2010). Experimental FRP/SRP–historic masonry delamination. *Composite Structures*, 92:891–903. doi: 10.1016/j.compstruct.2009.09.029

Corradi, M., Di Schino, A., Borri, A., Rufini, R. (2018). A review of the use of stainless steel for masonry repair and reinforcement. *Construction and Building Materials*, 181:335–346. doi: 10.1016/j.conbuildmat.2018.06.034

Corradi, M., Granizi, A., Borri, A. (2007). Confinement of brick masonry columns with CFRP Materials. *Composites Science and Technology*, 67:1772–1783. doi: 10.1016/j.compscitech.2006.11.002

Cressman, E. R. (1962). The data of Geochemistry: Chapter T. Nondetrital Siliceous Sediments. Washington: United States Government Printing Office.

Flower, M. F. (1973). Evolution of basaltic and differentiated lavas from Anjouan, Comores Archipelago. *Contributions to Mineralogy and Petrology*, 38:237–260. doi: 10.1007/bf00374768

Geyve. (2022). Ali Fuat Paşa Köprüsü. http://www.geyve.gov.tr/ali-fuat-pasa-koprusu (Accessed date: 01.11.2022)

Geyveyoresi. (2022). https://geyveyoresi.com/alifuatpasa-koprusu-kemerleri-1923-mubadele-doneminde-muhacirler-tarafindan-barinak-olarak-kullanildi/ (01.11.2022)

Ghalamghash, J., Mirnejad, H., Rashid, H. (2009). Mixing and mingling of mafic and felsic magmas along the Neo-Tethys continental margin, Sanandaj-Sirjan Zone, NW Iran: A case study from the Alvand Pluton. *Neues Jahrbuch für Mineralogie – Abhandlungen*, 186:79–93. doi: 10.1127/0077-7757/2009/0133

Grande, E., Imbimbo, M, Sacco, E. (2011). Bond behavior of historical clay bricks strengthened with steel reinforced polymers (SRP). *Materials*, 4:585–600. doi: 10.3390/ma4030585

Halden, N. M., Bowes, D. R. (1984). Metamorphic development of cordierite-bearing layered schist and mica schist in the vicinity of Savonranta, Eastern Finland. *Bulletin of the Geological Society of Finland*, 56:3–23. doi: 10.17741/bgsf/56.1-2.001

Kesonen, A. (2015). Mechanical properties of Finnish rocks based on uniaxial compressive strength and tensile strength tests. Master's Thesis, Degree Programme in Structural Engineering and Building Technology, School of Engineering, Aalto University.

Mihladiz, N. S., Sancak, E. (2015). Sakarya ili Ali Fuat Paşa Köprüsü (II. Bayezid Köprüsü) üzerinde Oluşan Yapısal Değişiklikler üzerine Bir Araştırma. *Süleyman Demirel Üniversitesi Fen Bilimleri Enstitüsü Dergisi*, doi: 10.19113/sdufbed.00783

Miskovsky, K., Seiki, T. (2011). Effect of heat on the mechanical properties of selected rock types – a laboratory study. *Harmonising Rock Engineering and the Environment*, 815–820. doi: 10.1201/b11646-149

Proske, D., Gelder, P. V. (2009). Safety of Historical Stone Arch Bridges, Berlin, Germany: Springer Press. doi: 10.1007/978-3-540-77618-5

Schultz, R. A. (1995). Limits on strength and deformation properties of jointed basaltic rock masses. *Rock Mechanics and Rock Engineering*, 28:1–15. doi: 10.1007/bf01024770

Varro, R., Bögöly, G., Görög, P. (2021). Laboratory and numerical analysis of failure of stone masonry arches with and without reinforcement, *Engineering Failure Analysis* 123 (2021) 105272, doi: 10.1016/j .engfailanal.2021.105272

Zhang, X-P., Wong, L. N., Wang, S-J., Han, G-Y. (2011). Engineering properties of quartz mica schist. *Engineering Geology*, 121:135–149. doi: 10.1016/j.enggeo.2011.04.020

Zhu, J., Bao, W., Peng, Q., Deng, X. (2020). Influence of substrate properties and interfacial roughness on static and dynamic tensile behaviour of rock-shotcrete interface from Macro and micro views. *International Journal of Rock Mechanics and Mining Sciences*, 132:104350. doi: 10.1016/j.ijrmms.2020.104350.